EMS602U

CFD Coursework

Flow over a compressor stator – Influence of the mesh and the numerical method

Group StarCCM G50

Shannen Venethethan ID : 210478226

Hossein Farahbakhsh, ID : 210438426

Tarren Sailesh Damji Popat, ID : 210394786

Abireshkanth Gnanakumar, ID : 210460232

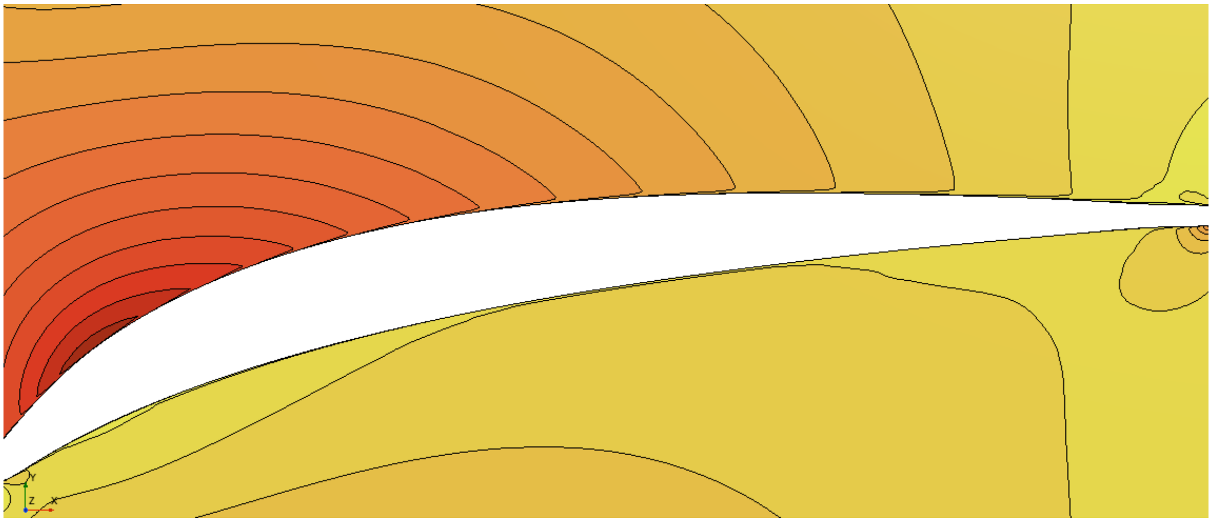

Abstract

This study investigated how different mesh resolution in a Computer Fluid Dynamic (CFD) simulation to analyse the flow characteristic over a compressor stator blade changes the predefined output parameters. Those being Axial and circumferential coefficients of force as well as the total pressure in the system. To produce valid results, 4 meshes were used coarse, medium, fine and other, all the meshes were run in the first and second order configurations. The results showed there is a clear trend between mesh resolution and accuracy of solution, meaning the finer the mesh, the more accurate at the cost of computational power. The other mesh on the other hand combines the finer mesh in critical regions, and the coarser mesh in areas of lower interest produced the lowest percentage error against the theoretical value of pressure at 2.74%, while being computationally less expensive to run. This highlights its viability for prototyping in industrial applications. In conclusion this study highlights the importance of mesh design and optimization for reliable Computer Fluid Dynamic (CFD) simulation, in this specific case for a compressor stator blade.

Table of Contents

1 Introduction

For an improved design and efficiency of the turbomachinery components, it is crucial to gain a good insight of the flow characteristics over a compressor stator. Computational Fluid Dynamics (CFD) is a powerful tool that is used to analyse the behaviour of flows and how they interact with various objects. In this report, the effect of various mesh resolutions (course, medium, fine, other) with varying calculation methods (first and second order) were studied. This was done by investigating the effect of a 2D flow on a turbine stator blade and analysing measurements such as axial force coefficients, circumferential force coefficients, static pressure, total pressure, and velocities along the stator blade. The stator blade's profile acted as a wall boundary preventing the flow from going through the blade.

1.1 Flow Physics

Many of the observations identified in this report were based on the Bernoulli equation which states that for an incompressible, steady flow, the total mechanical energy (pressure, kinetic, and potential energy) along a streamline is constant and is expressed as:

$$P + \frac{1}{2}\rho V^2 + \rho g h = constant \quad (1)$$

Where P is pressure, V is velocity, and h is height. This principle helps analyse fluid flow in various engineering applications.

The selection of numerical method of solution to the governing equations also has a key impact in the correct capturing of the flow over the stator. The solvers apply Reynolds Averaged Navier-Stokes (RANS) to simulate the turbulent flow; the turbulence closes using models such as k-ε and SST turbulence models. (Menter, (1994)) It is possible to add artificial viscosity terms to stabilize a numerical solution, especially in zones where flow is non-stationary or shocks are initiated. However, it is imperative not to over-smooth the field since elevated levels of viscosity synthesis artificially change the flow physics.

1.2 Flow Behaviour

The dominant type of flow in such systems is viscous which may be characterized by varying velocities and pressures across the boundary layers and wake. This behaviour in-flow is manifested in a dramatic dependence on the boundary conditions that determine the flow interaction with the stator surface. This boundary layer develops at the surface of the stator blades and thereby affects the velocity-pressure distribution. (Schlichting, (2000).) But at certain conditions, particularly when the pressure gradient is high enough, flow separation may take place. This separation may give rise to recirculating flow regions believed to depress the operating efficiency of the compressor. (Versteeg, (2007).)

1.3 Accuracy of Results

Among the factors affecting the accuracy of the computational results, meshing is one of the most significant features because by refining the mesh, one can accurately resolve the boundary layer and separation zones; whereas a coarse mesh might not at all resolve these characteristics. (Ferziger, (2002)) A mesh with better resolution would enhance the accuracy of the simulation though mesh convergence and is often checked by the method of residuals and making sure that to some degree they are low enough.

1.4 Flow Parameters & Solver Settings

The stator blade was set at a whirl angle of 41° ad the inlet flow velocity was set to 35 m/s in the positive x-direction. The flow was assumed to be inviscid and incompressible. A constant density of 1.225 kg/m³ was set for the fluid (Air). The inlet was set to a constant total pressure of 870 Pa. The stopping criteria, minimum limits, and maximum limits were also set before the simulations were ran. The simulations were run until the residuals were converged to ensure the results that were found were accurate and consistent to at least 3 significant figures.
The important solver settings consist of time scale selection between steady-state and transient

analysis, selection of turbulence models, and convergence criteria. (Patankar, (1980)) The numerical setup should be such that makes it possible to be repeated in other software systems. For this study, a structured mesh will be used to capture the flow details especially at the vicinity of the wall and wake regions. The convergence analysis will be carried out to check that the overall results are not mesh dependent. During the simulation, the values of residuals and mesh should be checked to see whether the solution is physically reasonable.

2 Methodology

This study required the simulation of a compressor stator blade subjected to an inviscid, steady, incompressible flow, to evaluate how mesh refinement and numerical discretion accuracy affect the values obtained for the axial and circumferential forces.

2.1 Geometry and mesh types

The compressor blade was a two-dimensional shape that was evaluated using a sequence of meshes (coarse, medium and fine), another mesh, and with the use of both first and second-order numerical discretions.

2.2 Flow

The stator blade was subjected to an inviscid steady incompressible flow with a constant density of 1.225 Kg/m^3, which was evaluated using the SIMPLE discretisation scheme (Semi-Implicit Method for Pressure-Linked Equations), where momentum and continuity equations were computed in a segregated flow manner. The flow was set initial conditions for pressure and velocity as the state of the flow field must be defined before attempting to compute the first iteration. These were 0 in all directions (X, Y, Z) for the value of pressure, but the X component of the velocity was made 10 m/s with Y and Z remaining 0 m/s for the axial report while for the circumferential report Y was set 10 m/s and X and y was set to 0 m/s.

2.3 Boundary conditions

Boundary conditions were set for the stator blade to govern the flow behaviour at the boundaries of the test subject. The boundaries created were a wall where the fluid cannot pass through the surface but can slide past the surface; a pressure inlet of 870 Pa; a pressure outlet of 0 Pa and a whirl angle of 41°.

2.4 Circumferential and axial force coefficients

To obtain values of the circumferential and axial force coefficients, equations must be set up. This was done using a reference velocity of 35 m/s and a blade reference area of 0.0294 m^2.

2.5 Monitors, solvers and stopping criteria

To assess residual convergence and coefficients of force, monitor plots were used, this allowed us to view any oscillatory behaviour within the continuity and momentum residuals, these were controlled by the use of the logical rule 'AND' or 'OR' to avoid the solver from terminating prematurely. Stopping criteria were used to determine the length of the simulation run time, to keep the simulation efficient and accurate. Circumferential and axial forces were monitored to observe any fluctuation in convergence and if changes were seen in the values of interest the threshold would be reduced until reaching a constant with three significant figures. The original threshold for the residual convergence was, 1×10^{-4} however, we ran the residuals until reaching convergence, which reduced the threshold to 1×10^{-15} when higher levels of precision were needed.

2.6 Post-processing

After processing the results, it was time to inspect them, this was done by creating pressure and velocity contours as well as velocity vectors. This allowed us to compare the contour lines of both orders of discretion alongside comparing against other mesh types. A more accurate method of doing this was to create an XY profile of pressure and velocity on the aerofoil.
By following these steps, the simulations were consistently validated, and convergence was assured under varying mesh densities and discretization schemes. This methodology ensures repeatability and transferability, allowing colleagues using different CFD software to replicate the setup.

3 Results

3.1 Effect of mesh refinement and 2nd order accuracy

Table 4 and Table 6 show that the velocity magnitudes at the leading and trailing edges are low, identified by the blue colour in those areas and signifying the stagnation points of the stator blade. This is expected and is due to the Bernoulli equation which states that for an incompressible, steady, non-viscous fluid, as the pressure at a point increases the velocity would decrease, further illustrated by Table 7 and Table 9.This is further proven by the fact that the contour lines are more packed at the stagnation points which indicates that there is a steep velocity gradient at those points. Table 4, Table 5, and Table 6 all show that as the meshes become more refined, the contour lines become smoother, indicating that the results are becoming more accurate.

A wake can be seen at the trailing edge of the stator blade (Table 6). This can be expected normally due to the viscosity of fluids, but in this case, since the flow is inviscid there should not be any viscous effects. Therefore, the presence of these wakes can be attributed to artificial viscosity that occurs in simulations. This reasoning can be further supported by the fact that as the mesh size decreases the effects of artificial viscosity get reduced, as seen in Table 6 showing the wake size decreasing with increasing mesh refinement.

Table 5 illustrates that the velocity magnitude at the top surface of the blade is higher than that of the bottom surface. This can be explained due to the upper surface having a longer length and therefore the fluid has to cover a larger distance at the top of the blade. Returning to Bernoulli's equation, this means the pressure at the top of the blade is lower than the bottom.
This can be further illustrated in Table 8 that shows that the top of the blade has lower values of pressure than the bottom, which causes the blade to move upwards and spin the turbine.

Figure 7 shows two peaks in pressure along the blade, indicating two stagnation points as seen previously in Table 4 and Table 6. Additionally, Figure 7 shows that as the mesh refinement increases, the number of points on the graph increases, thus making the solution more accurate.
Since Bernoulli's equation states that the total pressure should remain constant for the simulation, Figure 6 shows that meshes calculated using the second order were more accurate since they had the straightest and flattest lines compared to first order simulations.

3.2 Comparison of 'other' vs. 'sequence' simulations

Firstly, to compare the other mesh it is empirical that it is compared to the sequence mesh that is most like it, this is in this case the medium mesh as it contains the exact same number of nodes in its mesh.

It can be agreed that there is a differentiation between the two meshes as even though they contain the same number of cells the two look completely different. The sequence medium mesh is structural and keeps its cell sizes evenly distributed. This is in complete contrast to the "other" mesh which has a higher number of smaller cells closer to the profile. As the cells near the profile are smaller, there is more area for the cells to perform approximations for the pressure. Which is exactly what the finer mesh does.

However, the “other” mesh maintains its bigger size in the non-populated areas like the coarse mesh (Fig 1,2).

This yields closer results to the finer mesh without being as computationally intensive. This, in industry is used for prototyping as less resources are needed therefore more iterations can be run. It also avoids the need to probe the area of low interest.

As mentioned, the smaller the cell and the more nodes the longer it takes to compute so although the finer mesh yields the most accurate results when taken to the extremes it would not be viable hence using the “other” mesh that has enhanced resolution in the profile would be the best option.

If the focus of the study however is to analyse the coefficient of circumferential the other mesh is deemed to be inaccurate compared to the sequence meshes since it does not have finer meshes near the outer walls as they are considered areas of low interest.

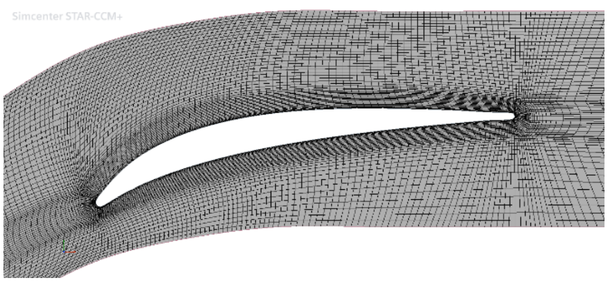

Figure 1: Other mesh

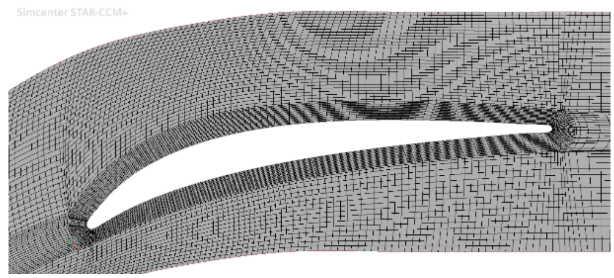

Figure 2: Medium mesh

3.3 Quantitative comparison of total pressure, force coefficients

Table 1: Compiled result for Circular and axial force coefficients

Mesh	Coefficient of force axial	Coefficient of force Circumferential	Cells
Coarse	-2.736458776	6.005453101	4095
Medium	-2.772970267	5.997204939	14754
Fine	-2.794866616	6.091311218	61356
Other	-2.765317462	5.831657761	14754

From Table 1, a clear trend can be seen as the finer the mesh becomes , the higher the Coefficient of circumferential force gets, indicating there are areas closer to the outer walls that when probed with a coarser mesh average out to a smaller value whereas with the finer mesh we can see that it yield a higher value. This trend concords with the fact that a higher amount of force is expected to be exerted on the outer wall. This means with an even finer mesh it can be expected to converge to the actual physical value.

A similar but opposite trend can also be observed for the Coefficient of axial force as the mesh size decreases the coefficient of force also decreases meaning that the smaller the mesh gets, the closer it will be to the true physical value.

It can be observed that the “other” mesh is slightly less accurate than the medium mesh overall for both values, but it achieves a similar result while necessitating significantly lower processing power.

This can be observed in the plots below Figure 3 ,4

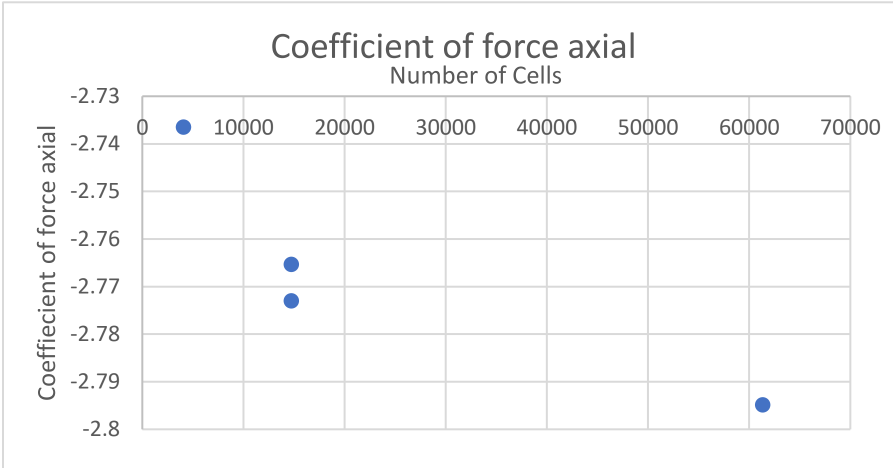

Figure 3. Plot of Coefficient of force axial

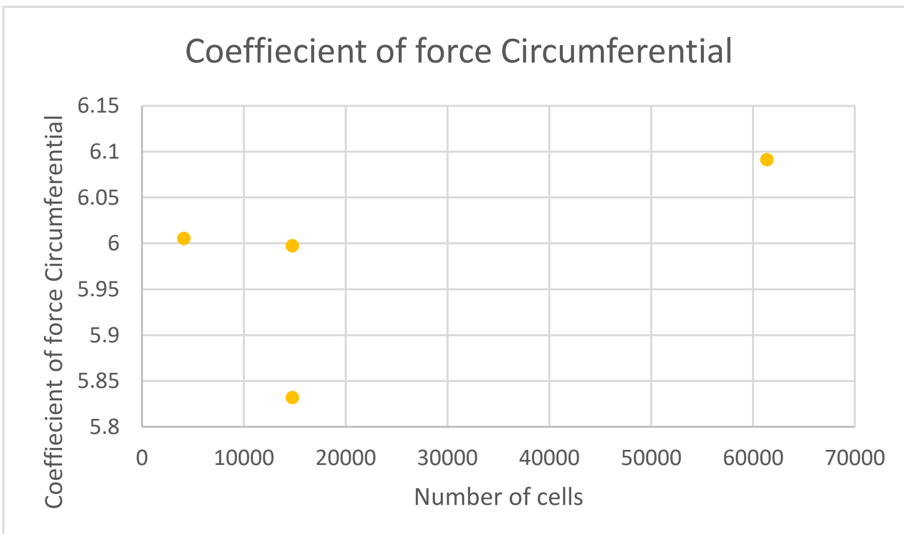

Figure 4. Plot of Coefficient of force axial

From section 1 it is known that the formula for the Bernoulli effect is:

$$P + \frac{1}{2}\rho V^2 + \rho g h = constant \quad (1)$$

However, in this study, we have designated some parameters that allow us to manipulate the above formula to find total pressure:

$$Total\ Pressure = \frac{1}{2}\rho V^2 \quad (2)$$

This is essentially the formula for kinetic energy which under no losses will give us the ideal total pressure for the system as all the force input in the system is converted to Pressure force.
The theoretical force in this case is 750.3125 Pa.

The total pressure for each instance was then calculated by averaging the total pressure values exported from each simulation. Below are tabulated values for total pressure for each instance and in a separate table the percentage error compared to the theoretical value for the second order including a bar graph.

Table 2: Total pressure for all instances simulated.

Mesh	Total Pressure (Pa)	
	1st order	2nd order
Coarse	522.8063784	557.4837185
Medium	586.4299911	687.5207033
Fine	682.1111331	780.9764597
Other	611.04714	729.7688188
Theoretical	750.3125	

Table 3. 2nd Order percentage error compared to theoretical

Mesh	2nd order	Percentage Error (%)
Coarse	557.4837185	25.69979595
Medium	687.5207033	8.36875258
Fine	780.9764597	4.086825116
Other	729.7688188	2.738016658
Theoretical	750.3125	

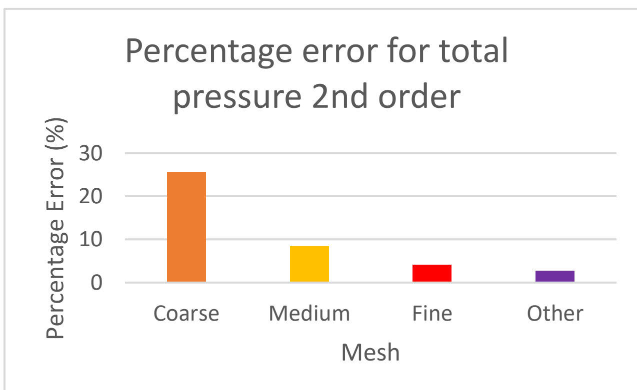

Figure 5. 2nd Order percentage error compared to theoretical bar chart.

From Figure 5, it can be observed there is a correlation between mesh size and reduction of percentage error when looking at Total pressure. However, the other mesh seems to be higher accuracy than the fine mesh. It should also be noted in Table 2,3 the algorithm using the fine mesh overestimates the value of total pressure in comparison to the closer other mesh value.

4 Summary

This study analysed the effects that varying mesh types and numerical discretion methods have on the accuracy and precision of values calculated during a compressor stator blade flow simulation. This experiment was carried out on a stator blade subjected to an 870 Pa air flow at a 41° whirl angle and simulated on StarCCM software. The simulations were run until the residuals converged, after which, key values and graphs were obtained such as the force coefficients, static pressures, total pressures, velocity magnitude contour plots, and pressure contour plots.

It was found that there were two stagnation points on the blade: one on the leading edge and the other on the trailing edge, coinciding with Bernoulli's findings. Additionally, it was found that there was a pressure difference created across the top and bottom of the stator blade, which allows the blade to move and rotate the turbine. The presence of artificial viscosity was also detected and was found to decrease with increasing mesh refinement. Comparing the first and second order simulations showed that second order simulations provided more accurate results and more closely reflected what was expected based of the Bernoulli principle. It was also found that as the number of cells increased (increasing refinement), the values for axial and circumferential force coefficients were more accurate and came closer to the theoretical values calculated.

This study illustrated that finer meshes offer greater accuracy during simulations. However, this does come with higher computational and time costs. The 'other' mesh type coupled with the second-order discretion proved to perform the best, offering solutions closest to theoretical values and an error percentage of 2.74% showing a high level of accuracy. This mesh type outperformed the sequence mesh types by creating finer meshes in areas of interest whilst maintaining coarser meshes in other regions, providing high accuracy whilst requiring lower computing power. The results obtained highlighted the importance of using mesh refinement in CFD, for reliable and accurate results.

5 References:

Ferziger, J. H. &. P. M., (2002). *Computational Methods for Fluid Dynamics..* s.l.:Springer..

Menter, F. R., (1994). Two-Equation Eddy-Viscosity Turbulence Models for Engineering Applications. *AIAA,* pp. 1598-1605.

Patankar, S. V., (1980). *Numerical Heat Transfer and Fluid Flow..* s.l.: Hemisphere Publishing Corporation..

Schlichting, H. &. G. K., (2000).. *Boundary-Layer Theory. Springer..* s.l.:s.n.

Versteeg, H. K. &. M. W., (2007). . *An Introduction to Computational Fluid Dynamics: The Finite Volume Method..* s.l.: Pearson Education..

6 Appendix (All)

Table 4: Showing the contour plots of the velocity magnitude at the leading edge of the stator blade.

	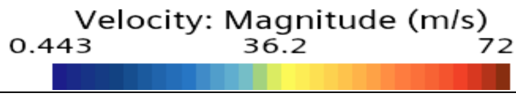	
	Leading Edge	
	First Order	Second Order
Course	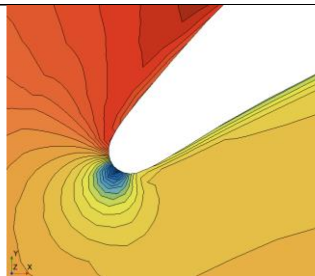	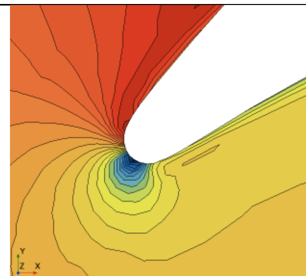
Medium	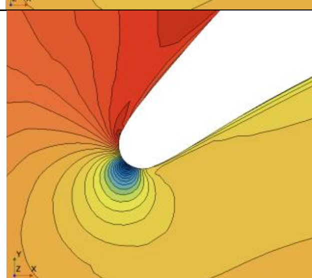	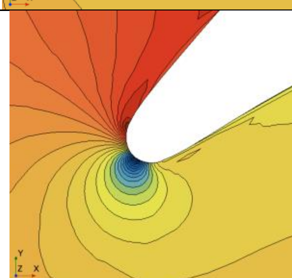
Fine	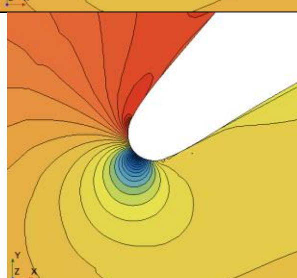	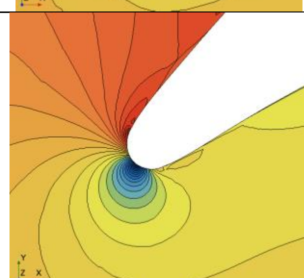
Other	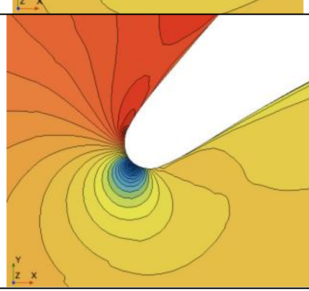	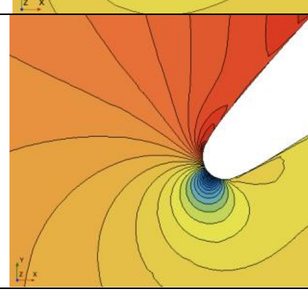

Table 5: Showing the contour plots of the velocity magnitude at the boundary layer of the stator blade.

	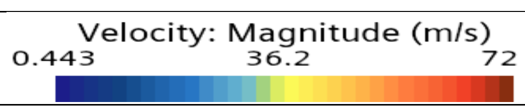	
	Boundary Layer	
	First Order	Second Order

Course	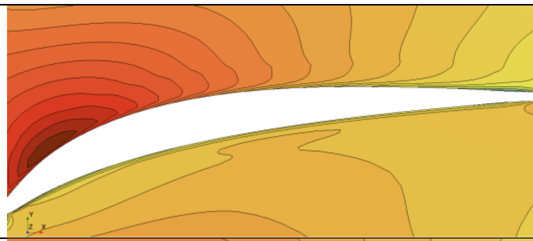	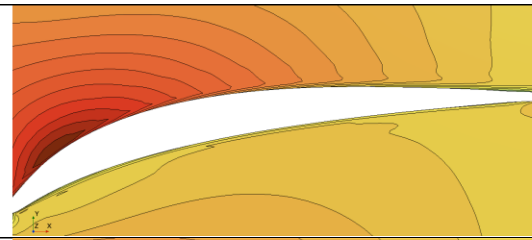
Medium	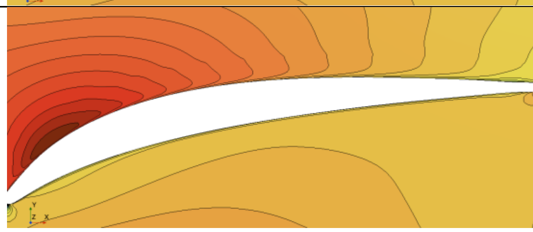	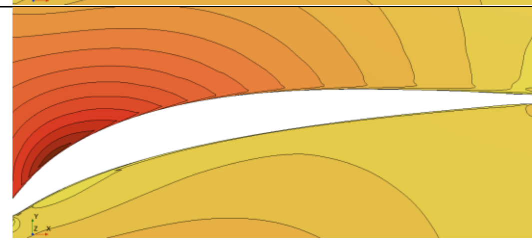
Fine	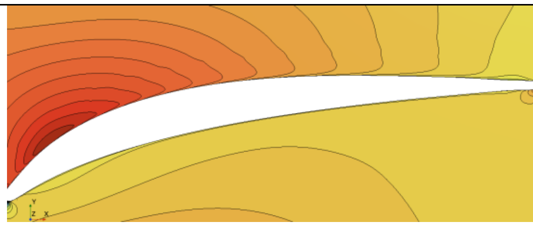	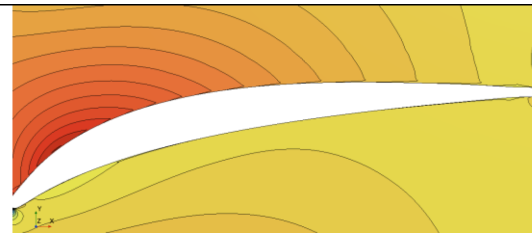
Other	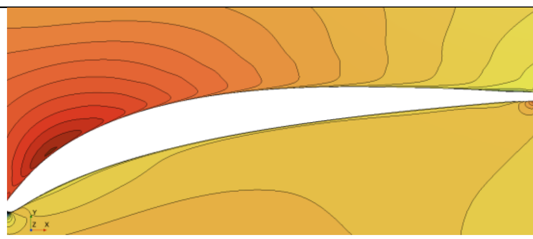	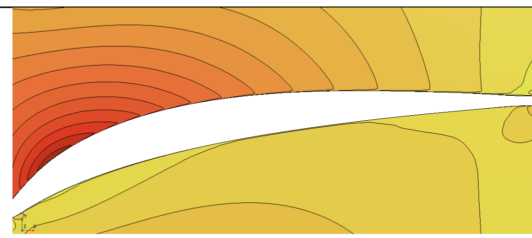

Table 6: Showing the contour plots of the velocity magnitude at the trailing edge of the stator blade.

	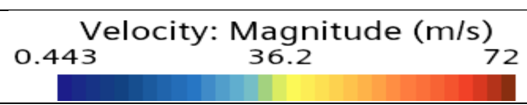	
	Trailing Edge	
	First Order	Second Order
Course	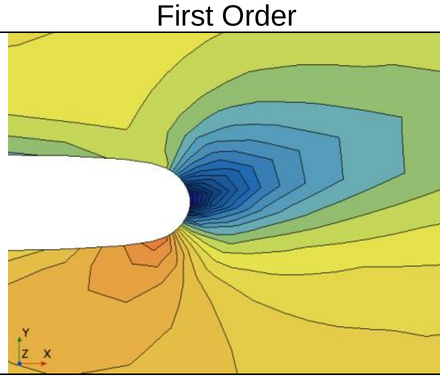	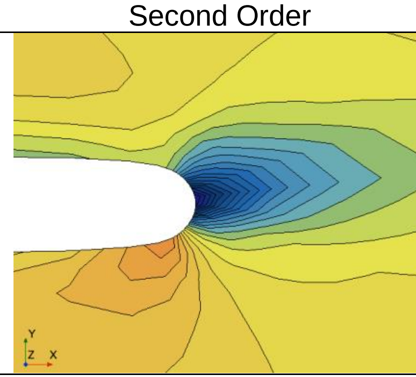

Medium	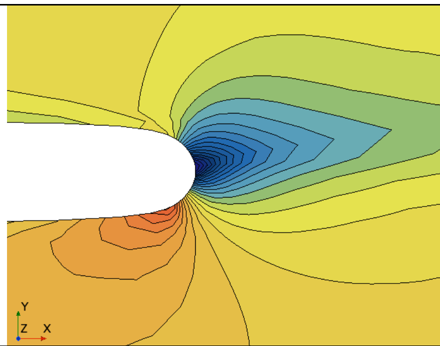	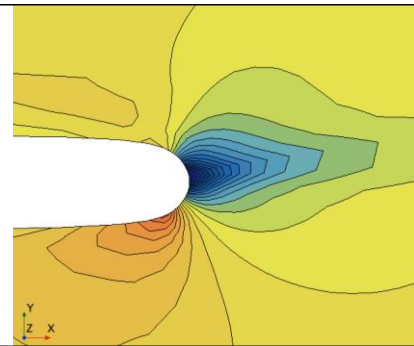
Fine	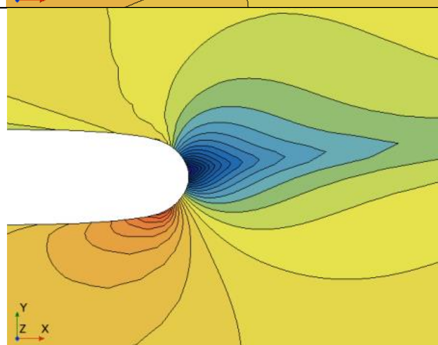	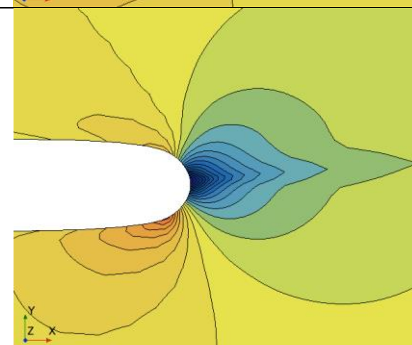
Other	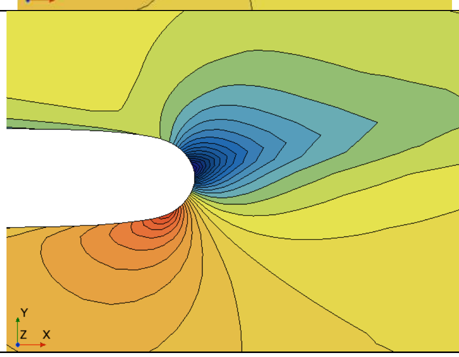	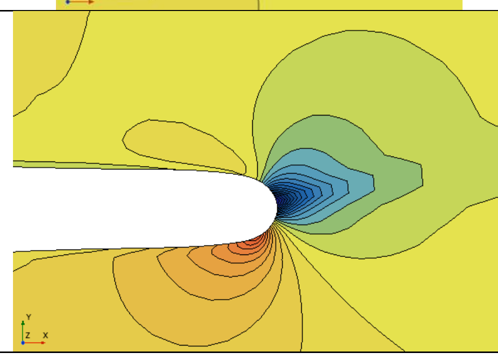

Table 7: Showing the contour plots of the pressure at the leading edge of the stator blade.

		
	Leading Edge	
	First Order	Second Order
Course	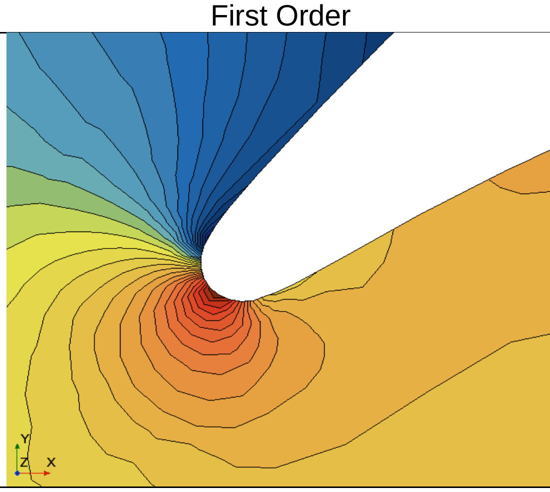	

Medium	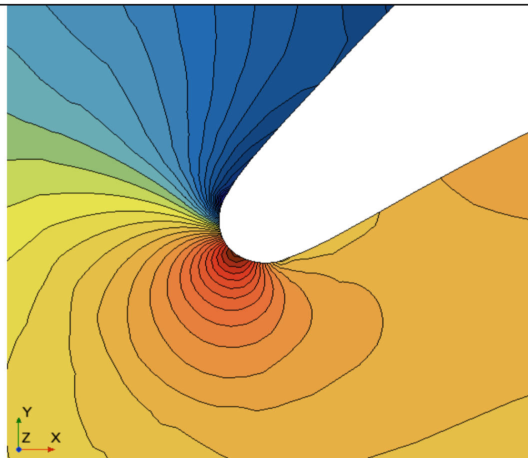	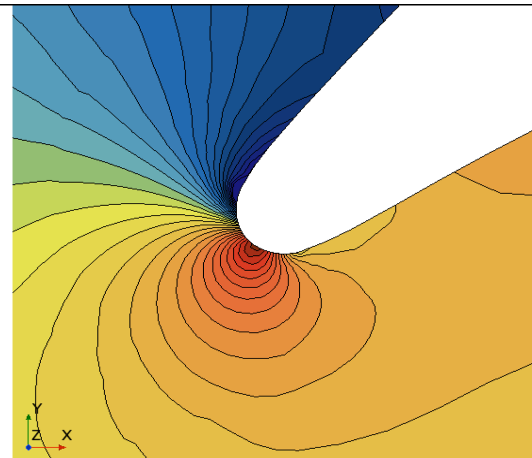
Fine	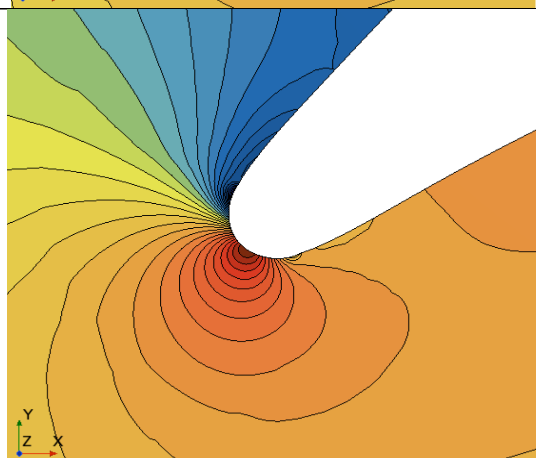	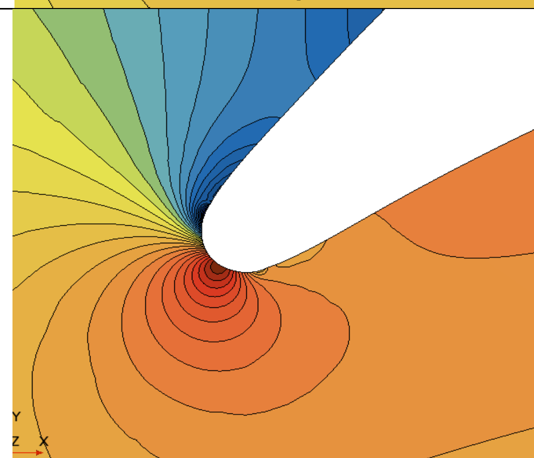
Other	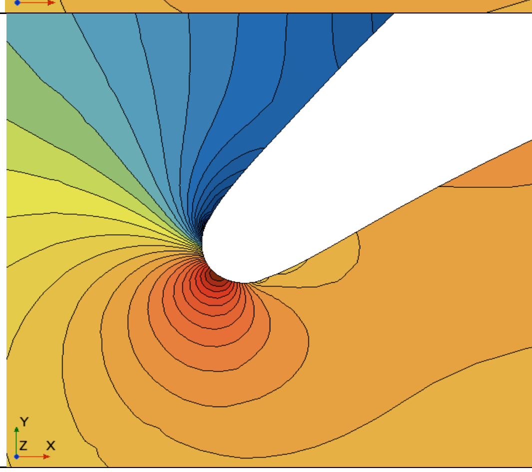	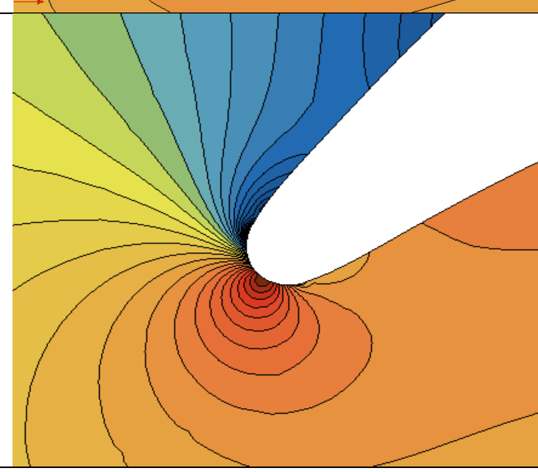

Table 8:Showing the contour plots of the pressure at the boundary layer of the stator blade.

	

	Boundary Layer	
	First Order	Second Order
Course	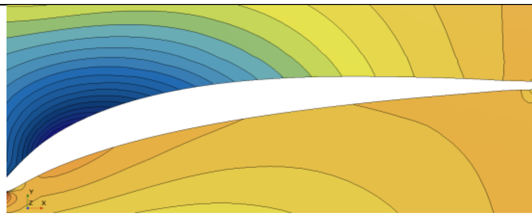	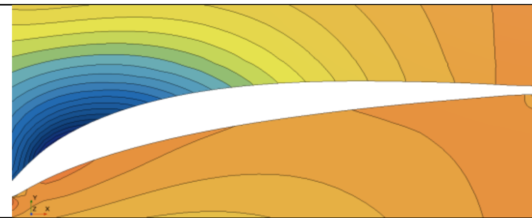
Medium	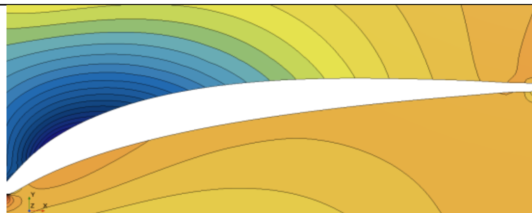	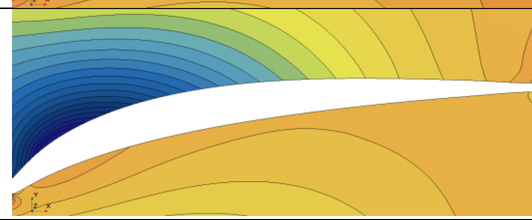
Fine	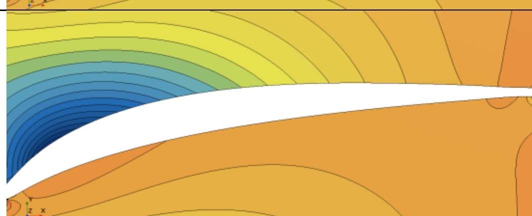	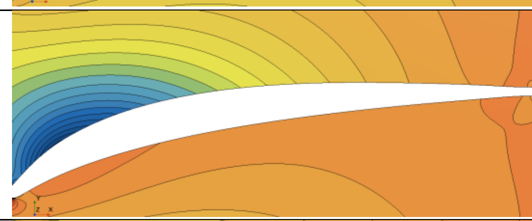
Other	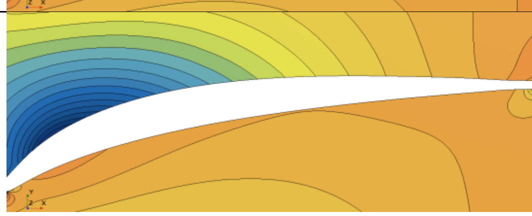	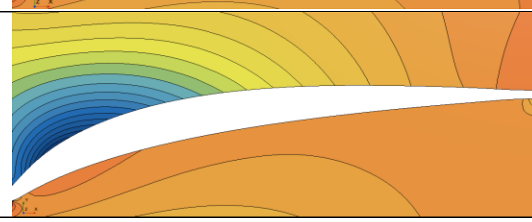

Table 9: Showing the contour plots of the pressure at the trailing edge of the stator blade.

		
	Trailing Edge	
	First Order	Second Order
Course	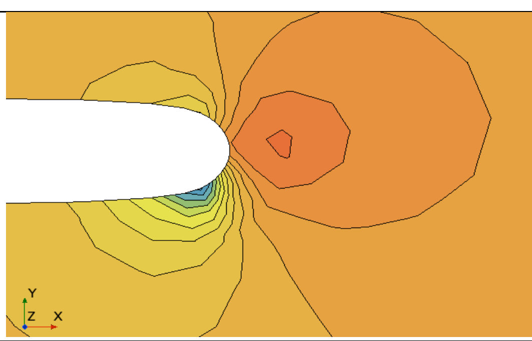	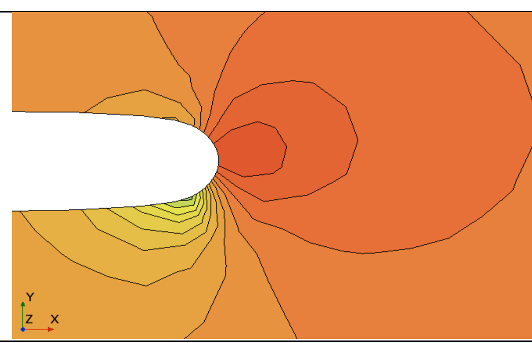

Medium	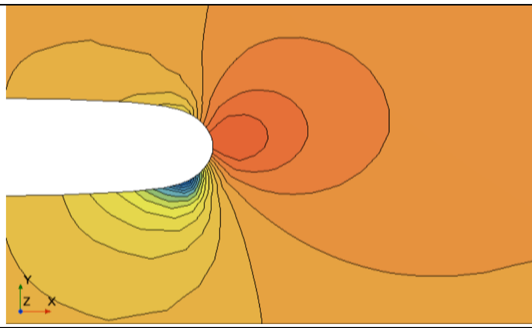	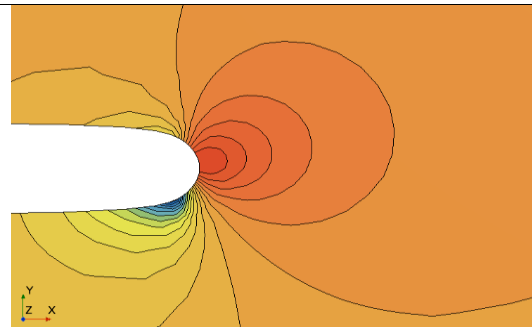
Fine	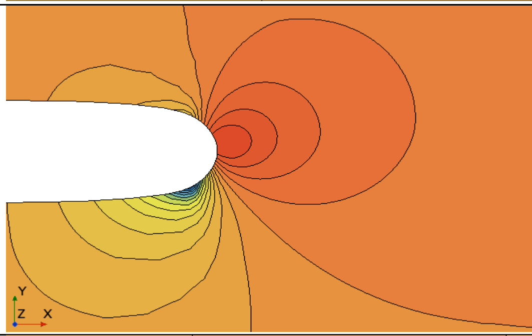	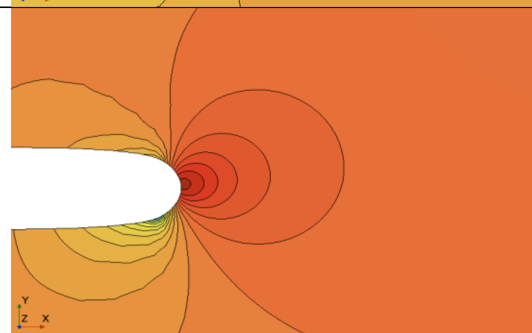
Other	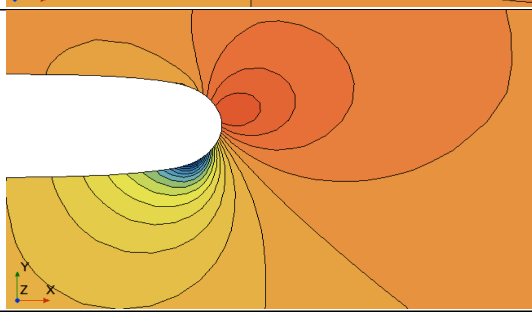	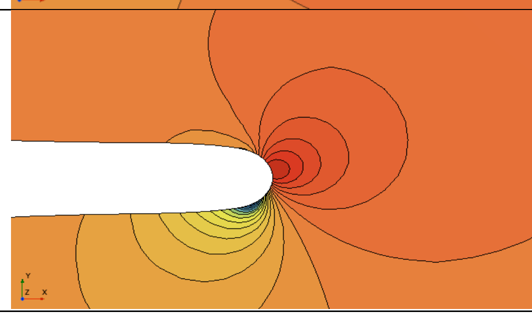

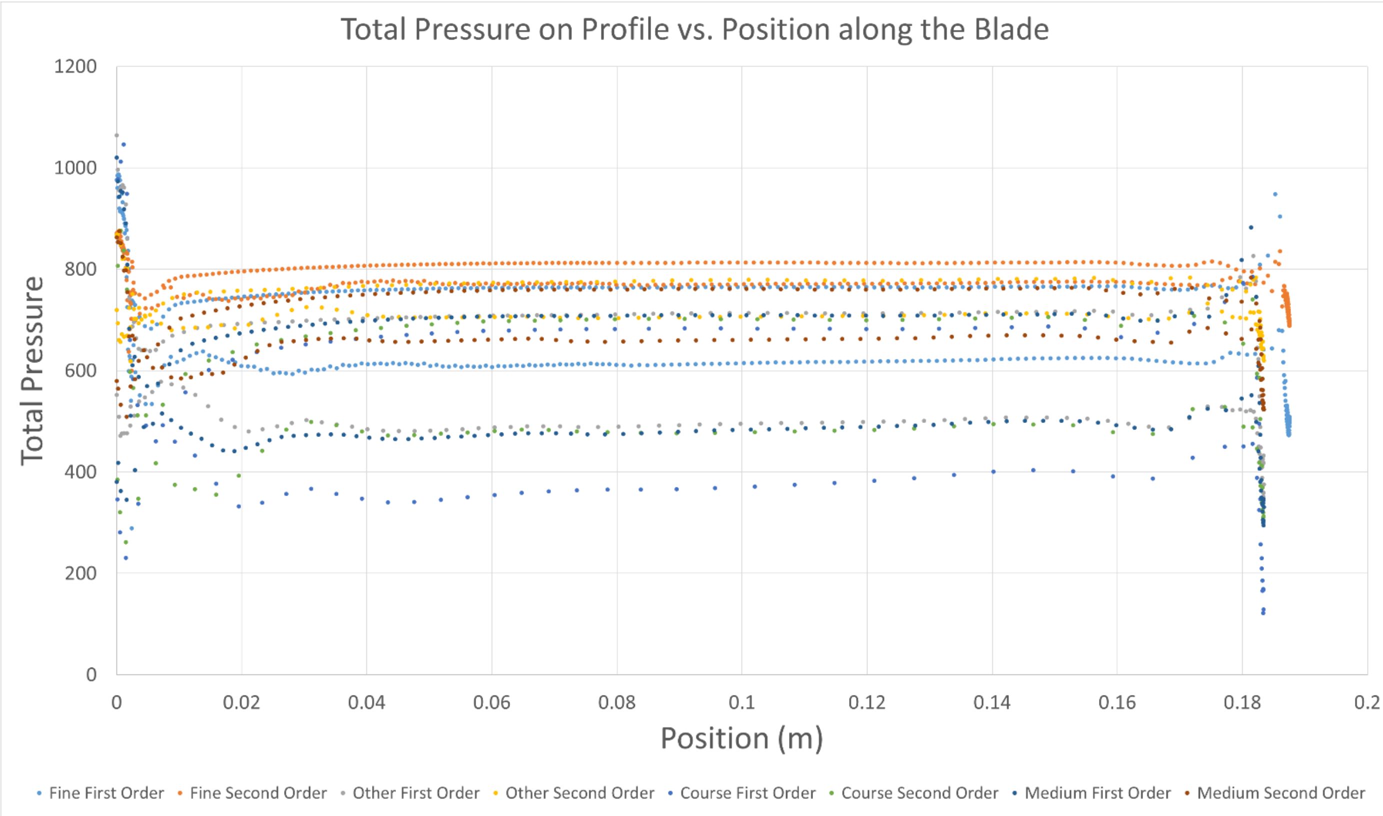

Figure 6: Showing the Total Pressure vs Position (m) graph along the stator blade.

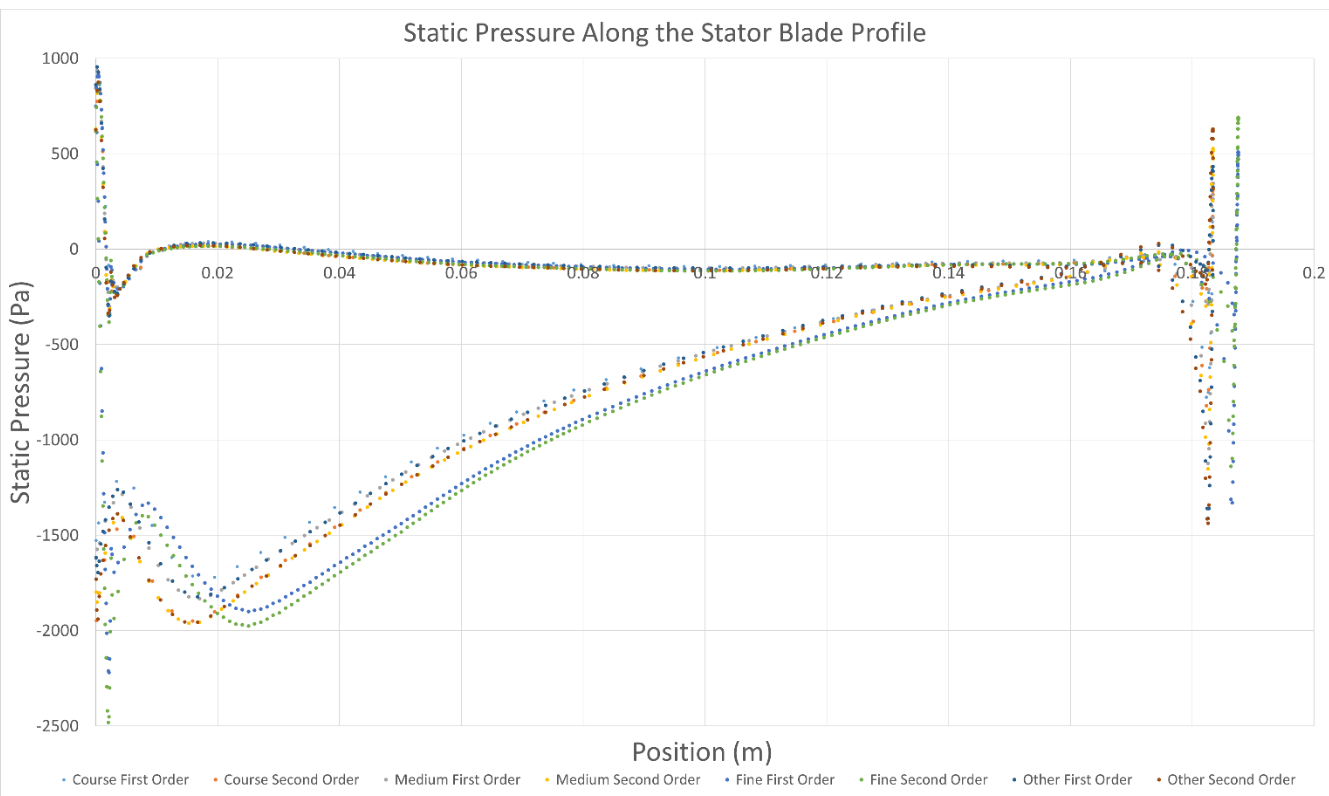

Figure 7: Showing the Static Pressure vs. Position (m) graph along the stator blade.